C. R. Mecanique 345 (2017) 832–843

Contents lists available at ScienceDirect

Comptes Rendus Mecanique

www.sciencedirect.com

Frequency analysis of a two-stage planetary gearbox using two different methodologies

Nabih Feki *, Maha Karray, Mohamed Tawfik Khabou, Fakher Chaari, Mohamed Haddar

Laboratoire de recherche de mécanique, modélisation et productique (LA2MP), École d'ingénieurs de Sfax, 3038 Sfax, Tunisia

ARTICLE INFO

Article history:
Received 20 June 2017
Accepted 6 October 2017

Keywords:
Lumped-parameter model
Phenomenological model
Two-stage planetary gear
Inertial reference frame
Rotating frame
Frequency analysis

ABSTRACT

This paper is focused on the characterization of the frequency content of vibration signals issued from a two-stage planetary gearbox. To achieve this goal, two different methodologies are adopted: the lumped-parameter modeling approach and the phenomenological modeling approach. The two methodologies aim to describe the complex vibrations generated by a two-stage planetary gearbox. The phenomenological model describes directly the vibrations as measured by a sensor fixed outside the fixed ring gear with respect to an inertial reference frame, while results from a lumped-parameter model are referenced with respect to a rotating frame and then transferred into an inertial reference frame. Two different case studies of the two-stage planetary gear are adopted to describe the vibration and the corresponding spectra using both models. Each case presents a specific geometry and a specific spectral structure.

1. Introduction

Planetary gear sets are used commonly in many industrial, automotive, aerospace and wind turbine gearbox applications. The complexity of the dynamic behavior of the planetary gearbox (PG) has been actively investigated using a model based on experimental approaches. Two different kinds of models have been implemented so as to describe the vibrations generated: PG (*i*) lumped-parameters models, and (*ii*) phenomenological models. The lumped-parameter models found in the literature describe the vibrations of all degrees of freedom referenced with respect to a rotating frame fixed to the carrier plate. However, phenomenological models describe directly the vibrations as measured by a sensor fixed outside the fix ring gear, which is subjected to periodic variation in vibration amplitudes when the planets pass through this fixed sensor. The two types of models should highlight the amplitude modulation (AM) of vibration time histories and modulation sidebands in the frequency domain induced by the time-varying vibration transmission path.

For the first type of models, the first study is that of Cunliffe et al. [1] who developed a model with a 13-degree of freedom to analyze the frequencies and mode shapes with a single fixed carrier. Then, Saada and Velex [2] developed the equations of motion of the system by the Lagrange method. Later, many research works have been done by Lin and Parker [3,4] and Chaari et al. [5,6] to describe the modal analysis and the dynamic response of the system.

* Corresponding author.
E-mail address: fekinabih@gmail.com (N. Feki).

https://doi.org/10.1016/j.crme.2017.10.001

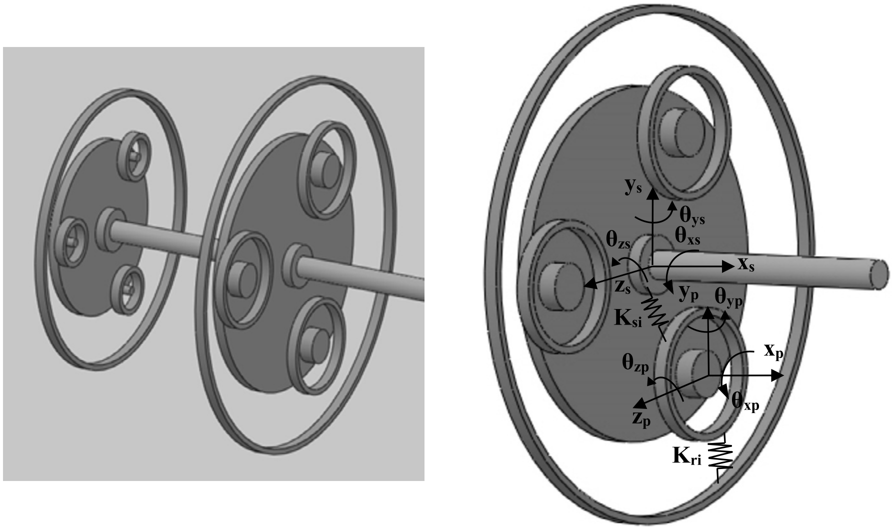

Fig. 1. Lumped parameter model of two stages planetary gear.

Concerning the second kind of models, McFadden and Smith [7] were the first to highlight the asymmetric distribution of modulation sidebands around mesh frequency and harmonics. Their model was able to predict the frequency content of the vibration signal issued from a planetary gear set. Later, McNames [8] explored the relative amplitudes of the dominant peaks using continuous-time Fourier series. Inalpolat and Kahraman [9] developed a simplified analytical model to describe the amplitude modulation of planetary gear sets. This model shows that there are different classes of planetary gear sets that exhibit different sideband behaviors. They also validated these trends through an experimental study. Molina [10] developed a phenomenological model that takes into account the variable vibration transmission paths through the ring gear and through the sun gear and carrier plate, something that had been missed in all previous publications. Samuel and Pines [11] described a technique based on the selection of an appropriate window function used to analyze the vibration signals collected from multiple sensors located around the ring gear. For the case of complex PG sets, one can find works dedicated to compound or multistage PG, which are based on lumped-parameter models. Thomas [12] developed an analytical model for investigating the transmission error and load distribution of a double helical gear pair. Zhang et al. [13] established a translational–rotational coupled dynamic model of a two-stage closed-form planetary gear set to predict the natural frequencies and vibration modes. Recently, Karray et al. [14] presented a complex configuration of a gearbox used in a bucket wheel excavator gearbox to investigate its modal properties. These models are difficult to implement and require a lot of care when computing the dynamic response. Phenomenological models can be an interesting alternative way to describe in a simple manner this behavior.

In this context, this paper will be concerned with developing two models of two-stage helical planetary gear using both the lumped-parameter model and the phenomenological model. Two case studies of two-stage planetary gear that differ from the point of view of geometry and assembly characteristics are developed, and the results obtained from each model will be presented and compared.

2. The lumped-parameter model

The studied gearbox is composed of a two-stage helical PG. Each stage is comprised, as shown by Fig. 1, of a ring gear (r) coupled with a sun gear (s) by N planets (P_n) and mounted on a carrier (c). All of these elements are considered as rigid bodies supported by elastic bearing. Meshing phenomena are approached by linear springs acting on the lines of action [15].

First, the equation of motion of each component is derived separately, and then assembled to obtain the overall system matrices of an N-planet helical PG train. Each component has six degrees of freedom: three translations (u_j, v_j and w_j) and three rotations (φ_j, ψ_j and θ_j, $j = \mathrm{c, r, s}, 1 \dots n$). These coordinates are measured with respect to a frame $(O, \vec{s}_1, \vec{t}_1, \vec{z}_1)$ fixed to the carrier and rotating with a constant angular speed Ω_c. The rotations (φ_j, ψ_j and θ_j) are replaced by their corresponding translational displacements as:

$$\rho_{jx} = R_{\mathrm{b}j}\varphi_j, \quad \rho_{jy} = R_{\mathrm{b}j}\psi_j, \quad \rho_{jz} = R_{\mathrm{b}j}\theta_j, \quad j = \mathrm{c, r, s}, 1, .., n \tag{1}$$

where $R_{\mathrm{b}j}$ is the base circle radius for the sun, the ring, the planet, and the radius of the circle passing through planet centers for the carrier. Circumferential planet locations are specified by the fixed angles α_i, which are measured relatively to the rotating basis vector $\vec{s}_1$, so that $\alpha_1 = 0$.

Then the coupling between the two stages is done using an additional torsional stiffness joining the rotational degree of freedom of the carrier wheel of the first stage and the sun gear of the second one and an additional linear spring joining the axial degrees of freedom of the same carrier and the sun.

The gyroscopic effect is neglected, since the considered gearbox is running at low speed.

The Lagrange formulation leads to the following equations of motion of the $2 \times (18 + 6N)$ degrees of freedom of the system:

$$M\ddot{q} + C\dot{q} + \left[K_{\mathrm{b}} + K(t)\right]q = F(t) \tag{2}$$

where q, M, C, K_{b}, K, F are respectively the displacement vector, the mass, the damping, the bearing, the mesh stiffness matrices and the external applied force vector. They are given, respectively, as follows:

$$q = \begin{Bmatrix} q_1 \\ q_2 \end{Bmatrix} \tag{3}$$

$$q_i = \begin{Bmatrix} u_{\mathrm{c}}, v_{\mathrm{c}}, w_{\mathrm{c}}, \rho_{\mathrm{c}x}, \rho_{\mathrm{c}y}, \rho_{\mathrm{c}z}, u_{\mathrm{r}}, v_{\mathrm{r}}, w_{\mathrm{r}}, \rho_{\mathrm{r}x}, \rho_{\mathrm{r}y}, \rho_{\mathrm{r}z}, u_{\mathrm{s}}, v_{\mathrm{s}}, w_{\mathrm{s}}, \rho_{\mathrm{s}x}, \rho_{\mathrm{s}y}, \rho_{\mathrm{s}z}, \\ u_1, v_1, w_1, \rho_{1x}, \rho_{1y}, \rho_{1z}, \ldots, u_n, v_n, w_n, \rho_{nx}, \rho_{ny}, \rho_{nz} \end{Bmatrix}^{\mathrm{T}} \tag{4}$$

q_1 is the degree of freedom vector of the first-stage planetary gear and q_2 is the degree of freedom of the second-stage planetary gear.

$$M = \mathrm{diag}(M_{\mathrm{c}1}, M_{\mathrm{r}1}, M_{\mathrm{s}1}, M_{11}, \ldots, M_{N1}, M_{\mathrm{c}2}, M_{\mathrm{r}2}, M_{\mathrm{s}2}, M_{12}, \ldots, M_{N2}) \tag{5}$$

$$\text{with } M_{ji} = \mathrm{diag}\left(m_{ji}, m_{ji}, m_{ji}, I_{jix}/R_{\mathrm{b}ji}^2, I_{jiy}/R_{\mathrm{b}ji}^2, J_{ji}/R_{\mathrm{b}ji}^2\right) \quad j = \mathrm{c}, \mathrm{r}, \mathrm{s}, 1, n, \ i = 1, 2 \tag{6}$$

diag denotes the diagonal matrix, m_{ji} is the mass, I_{jix} and I_{jiy} are the diametrical mass moments of inertia and J_{ji} is the polar mass moment of inertia of element j in stage i.

The bearing stiffness matrix K_{b} is written as:

$$K_{\mathrm{b}} = \mathrm{diag}(K_{\mathrm{bc}1}, K_{\mathrm{br}1}, K_{\mathrm{bs}1}, K_{\mathrm{b}11}, \ldots, K_{\mathrm{b}N1}, K_{\mathrm{bc}2}, K_{\mathrm{br}2}, K_{\mathrm{bs}2}, K_{\mathrm{b}12}, \ldots, K_{\mathrm{b}N2}) \tag{7}$$

$$\begin{cases} K_{\mathrm{b}ji} = \mathrm{diag}(k_{jix}, k_{jiy}, k_{jiz}, k_{ji\phi}, k_{ji\psi}, k_{ji\theta}); \quad j = \mathrm{c}, \mathrm{r}, \mathrm{s}, \ i = 1, 2 \\ K_{\mathrm{b}ni} = \mathrm{diag}(0, 0, 0, k_{ni\phi}, k_{ni\psi}, k_{ni\theta}); \quad n = 1, \ldots N \end{cases} \tag{8}$$

The gearmesh stiffness matrix is time varying. For a helical planetary gear, a trapezoidal waveform is adopted to express this variation [16]. It can be expressed by:

$$K(t) = \begin{bmatrix} K_{11} & 0 & 0 & K_{14}^1 & \ldots & K_{14}^n \\ 0 & K_{22}(t) & 0 & K_{24}^1(t) & \cdots & K_{24}^n(t) \\ 0 & 0 & K_{33}(t) & K_{34}^1(t) & \cdots & K_{34}^n(t) \\ K_{41}^1 & K_{42}^1(t) & K_{43}^1(t) & K_{44}^1(t) & 0 & 0 \\ \vdots & \vdots & \vdots & 0 & \ddots & 0 \\ K_{41}^n & K_{42}^n(t) & K_{43}^n(t) & 0 & 0 & K_{44}^n(t) \end{bmatrix} \tag{9}$$

$$K(t) = \begin{bmatrix} \sum K_{\mathrm{c}11}^n + K_{\mathrm{c}} & 0 & 0 & K_{\mathrm{c}21}^1 & \cdots & K_{\mathrm{c}21}^N & 0 & 0 & -K_{\mathrm{c}} & 0 & \cdots & 0 \\ 0 & \sum K_{\mathrm{r}11}^n & 0 & K_{\mathrm{r}21}^1 & \cdots & K_{\mathrm{r}21}^N & 0 & 0 & 0 & 0 & \cdots & 0 \\ 0 & 0 & \sum K_{\mathrm{s}11}^n & K_{\mathrm{s}21}^1 & \cdots & K_{\mathrm{s}21}^N & 0 & 0 & 0 & 0 & \cdots & 0 \\ K_{\mathrm{c}21}^1 & K_{\mathrm{r}21}^1 & K_{\mathrm{s}21}^1 & K_{\mathrm{pp}1}^1 & 0 & 0 & 0 & 0 & 0 & 0 & \cdots & 0 \\ \vdots & \vdots & \vdots & 0 & \ddots & 0 & 0 & 0 & 0 & 0 & \cdots & 0 \\ K_{\mathrm{c}21}^N & K_{\mathrm{s}21}^N & K_{\mathrm{s}21}^N & 0 & 0 & K_{\mathrm{pp}1}^N & 0 & 0 & 0 & 0 & \cdots & 0 \\ 0 & 0 & 0 & 0 & \cdots & 0 & \sum K_{\mathrm{c}12}^n & 0 & 0 & K_{\mathrm{c}22}^1 & \cdots & K_{\mathrm{c}22}^N \\ 0 & 0 & 0 & 0 & \cdots & 0 & 0 & \sum K_{\mathrm{r}12}^n & 0 & K_{\mathrm{r}22}^1 & \cdots & K_{\mathrm{r}22}^N \\ -K_{\mathrm{c}} & 0 & 0 & 0 & \cdots & 0 & 0 & 0 & \sum K_{\mathrm{s}12}^n + K_{\mathrm{c}} & K_{\mathrm{s}22}^1 & \cdots & K_{\mathrm{s}22}^N \\ 0 & 0 & 0 & 0 & \cdots & 0 & K_{\mathrm{c}22}^1 & K_{\mathrm{r}22}^1 & K_{\mathrm{s}22}^1 & K_{\mathrm{pp}2}^1 & 0 & 0 \\ \vdots & 0 & 0 & 0 & \cdots & 0 & \vdots & \vdots & \vdots & 0 & \ddots & 0 \\ 0 & 0 & 0 & 0 & \cdots & 0 & K_{\mathrm{c}22}^N & K_{\mathrm{s}22}^N & K_{\mathrm{s}22}^N & 0 & 0 & K_{\mathrm{pp}2}^N \end{bmatrix} \tag{10}$$

where K_{c} is the coupling stiffness matrix:

$$K_{\mathrm{c}} = \mathrm{diag}(0, 0, K_{\mathrm{a}}, 0, 0, K_{\mathrm{t}}) \tag{11}$$

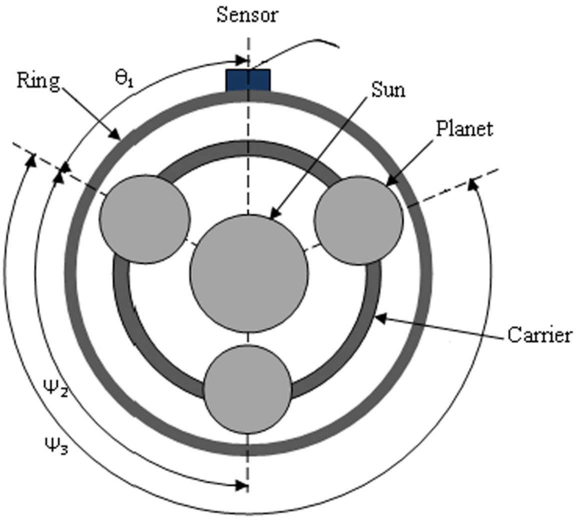

Fig. 2. Measurement arrangement on a single-stage planetary gearbox.

K_a and K_t denote, respectively, the axial coupling and the torsional coupling.

Based on Rayleigh's method, C is chosen to be proportional to M and the mean value of $K_b + K(t)$.

The external torques applied to the system are C_{ci}, C_{ri}, C_{si} on the carrier, the ring, and the sun (time constant), respectively. The corresponding forces are:

$$F(t) = \langle F_1(t), F_2(t) \rangle^T \tag{12}$$

$$\text{with } F_i(t) = \langle 0, 0, T_{ci}, 0, 0, T_{ri}, 0, 0, T_{si}, 0, \ldots, 0 \rangle^T \tag{13}$$

$$\text{and } T_{ji} = C_{ji}/r_{ji}, \quad j = \mathrm{c, r, s} \tag{14}$$

3. The phenomenological model

3.1. Vibration signal

The phenomenological model describes the vibrations as measured by the sensor fixed on the outer part on the ring gear (Fig. 2).

Planetary gear train vibrations are different from vibrations in parallel axis gear trains. They are complex to analyze, not only because there are multiple meshes with multiple planets producing similar vibrations, but also because of the variable distance between planet gears and the transducer's location. This variable distance creates a variable transmission path of the vibration, which is at the origin of a planet-pass modulation.

The vibrations $v_i^r(t)|I = 1, \ldots, N$ are considered periodic with fundamental frequency equal to the gear mesh frequency $f_p = Z_r f_c$ (where Z_r is the tooth number of the ring gear, and f_c is the carrier rotation frequency). It can be expressed by [10]:

$$v_i^r(t) = v_1^r(t - \gamma_{ri} T_p) \tag{15}$$

with $v_1^r(t)$ is the vibration generated on the meshing between the first planet and the ring gear, $\gamma_{ri} = \frac{\psi_i Z_r}{2\pi}$ is the relative phase difference, and $T_p = 1/f_p$ is the gear mesh period of the planetary gearbox.

The term ψ_i is the angle between the first planet gear and the i-th planet gear ($\psi_1 = 0$).

The amplitude modulation functions $a_i^r(t)$ are considered periodic with fundamental frequency equal to the carrier rotating frequency f_c. It can be expressed by:

$$a_i^r(t) = a_1^r\left(t - \frac{\psi_i T_c}{2\pi}\right) \tag{16}$$

where $a_1^r(t)$ is the amplitude modulation function of the first planet, taking into account the angular position of planet iψ_i and T_c the rotational period of the carrier.

In practice, the position of the planets is not known at the moment of measurement. It is represented in Fig. 2 by θ_1. To take into account the unknown position θ_1 of planet 1, a time shift $t_1 = \theta_1/2\pi f_c$ is introduced into the amplitude modulation functions.

$$a_i^{\mathrm{r}}(t) = a_1^{\mathrm{r}}\left(t - t_1 - \frac{\psi_i T_{\mathrm{c}}}{2\pi}\right) \tag{17}$$

The sensor measures the sum of all amplitude-modulated vibrations generated by the passage of the all planets; this measurement can be expressed as follows:

$$\begin{aligned} x_j^{\mathrm{r}}(t) &= \sum_{i=1}^{N} x_{ij}^{\mathrm{r}}(t) = \sum_{i=1}^{N} a_{ij}^{\mathrm{r}}(t) v_{ij}^{\mathrm{r}}(t) \\ &= \sum_{i=1}^{N_j} a_{1j}^{\mathrm{r}}\left(t - t_{1j} - \frac{\psi_{ij} T_{\mathrm{c}j}}{2\pi}\right) v_{1j}^{\mathrm{r}}(t - \gamma_{\mathrm{r}ji} T_{\mathrm{p}j}) \end{aligned} \tag{18}$$

with $j = 1$ for the first stage and $j = 2$ for the second one.

The interaction of the vibration generated between the two stages of the planetary gear is evidenced by a modulation between mesh frequencies [17,18]. So the mesh frequency of the first stage of the planetary gear is modulated by the mesh frequency of the second one, and it is expressed by:

$$x_1^{\mathrm{r}}(t) = \sum_{i=1}^{N_1} a_{11}^{\mathrm{r}}\left(t - t_{11} - \frac{\psi_{i1} T_{\mathrm{c}1}}{2\pi}\right) v_{11}^{\mathrm{r}}(t - \gamma_{\mathrm{r}1i} T_{\mathrm{p}1}) v_{12}^{\mathrm{r}}(t - \gamma_{\mathrm{r}2i} T_{\mathrm{p}2}) \tag{19}$$

For the second stage, the amplitude-modulated vibration generated is as follows:

$$x_2^{\mathrm{r}}(t) = \sum_{i=1}^{N_1} a_{12}^{\mathrm{r}}\left(t - t_{12} - \frac{\psi_{i2} T_{\mathrm{c}2}}{2\pi}\right) v_{12}^{\mathrm{r}}(t - \gamma_{\mathrm{r}2i} T_{\mathrm{p}2}) \tag{20}$$

3.2. Frequency analysis

The frequency analysis of Eq. (18) is carried out through the calculation of its Fourier transform (FT). The FT of equation (18) is given by:

$$\begin{aligned} X_j^{\mathrm{r}}(f) &= \sum_{i=1}^{N} X_{ij}^{\mathrm{r}}(f) \\ &= \sum_{i=1}^{N} \underbrace{\Im\left\{a_{1j}^{\mathrm{r}}\left(t - t_{1j} - \frac{\psi_{ij} T_{\mathrm{c}j}}{2\pi}\right)\right\}}_{\mathrm{I}} * \underbrace{\Im\left\{v_{1j}^{\mathrm{r}}(t - \gamma_{\mathrm{r}ji} T_{\mathrm{p}j})\right\}}_{\mathrm{II}} \end{aligned} \tag{21}$$

where $\Im\{.\}$ represents the FT, and $*$ represents the convolution product.

The term (I) of equation (21) can be expressed by:

$$a_{ij}^{\mathrm{r}}(t) = a_{1j}^{\mathrm{r}}\left(t - t_{1j} - \frac{\psi_{ij} T_{\mathrm{c}j}}{2\pi}\right) = \sum_{q \in z} \alpha_q^{\mathrm{r}} \mathrm{e}^{\mathrm{j}2\pi q f_{\mathrm{c}j}(t - t_{1j} - \frac{\psi_{ij} T_{\mathrm{c}j}}{2\pi})} \tag{22}$$

where α_q^{r} and $q \in z$ are the Fourier coefficients of $a_{ij}^{\mathrm{r}}(t)$.

Taking the FT of Eq. (22) and invoking its time-shifting property, the expression of term (I) yields:

$$\Im\left\{a_{1j}^{\mathrm{r}}\left(t - t_{1j} - \frac{\psi_{ij} T_{\mathrm{c}j}}{2\pi}\right)\right\} = \sum_{q \in z} \alpha_q^{\mathrm{r}} \mathrm{e}^{\mathrm{j}2\pi q f_{\mathrm{c}j}(t_{1j} + \frac{\psi_{ij} T_{\mathrm{c}j}}{2\pi})} \delta(f - q f_{\mathrm{c}j}) \tag{23}$$

with $\delta(z) = 1$ if $z = 0$ and $\delta(z) = 0$ if $z \neq 0$ (it is the Dirac delta).

The term (II) of equation (21) can be developed as follows:

$$v_{ij}^{\mathrm{r}}(t) = v_{1j}^{\mathrm{r}}(t - \gamma_{\mathrm{r}ji} T_{\mathrm{p}j}) = \sum_{k \in z} \beta_k^{\mathrm{r}} \mathrm{e}^{\mathrm{j}2\pi k f_{\mathrm{p}j}(t - \gamma_{\mathrm{r}ji} T_{\mathrm{p}j})} \tag{24}$$

with β_k^{r} and $q \in z$ are the Fourier coefficients of $v_{ij}^{\mathrm{r}}(t)$.

Taking the FT of equation (24), the expression of term (II) can be written by:

$$\Im\left\{v_{1j}^{\mathrm{r}}(t - \gamma_{\mathrm{r}ji} T_{\mathrm{p}j})\right\} = \sum_{k \in z} \beta_k^{\mathrm{r}} \mathrm{e}^{-\mathrm{j}2\pi k f_{\mathrm{p}j} \gamma_{\mathrm{r}ji} T_{\mathrm{p}j}} \delta(f - k f_{\mathrm{p}j}) \tag{25}$$

Substituting the expressions (23) and (25) into equation (19), using the sampling property of the Dirac delta, we obtain:

Table 1
Groups of planetary gear sets.

Group	Group description	Conditions		Effect on the spectra
		1	2	
(A)	Equally spaced planet gears and in-phase gear meshing	$\psi_{ji}=\frac{2\pi(i-1)}{N}$	$\gamma_{rji}=\frac{\psi_{ji}Z_{rj}}{2\pi}\in N$	Symmetric sidebands
(B)	Equally spaced planet gears and out-of-phase meshing	$\psi_{ji}=\frac{2\pi(i-1)}{N}$	$\gamma_{rji}=\frac{\psi_{ji}Z_{rj}}{2\pi}\notin N$	Asymmetric sidebands with no gear mesh frequency
(C)	Unequally spaced planet gears and in-phase meshing	$\psi_{ji}\neq\frac{2\pi(i-1)}{N}$	$\gamma_{rji}=\frac{\psi_{ji}Z_{rj}}{2\pi}\in N$	Symmetric sidebands with the same relative magnitude between the central component and its sidebands for all harmonics
(D)	Unequally spaced planet gears and out-of-phase meshing	$\psi_{ji}\neq\frac{2\pi(i-1)}{N}$	$\gamma_{rji}=\frac{\psi_{ji}Z_{rj}}{2\pi}\notin N$	Asymmetric and rich sidebands

$$X_1^{\mathrm{c}}(f)=\sum_{k\in z}\sum_{q\in z}\sum_{i=1}^{N_1}\alpha_q^{\mathrm{c}}\beta_k^{\mathrm{c}}\mathrm{e}^{-\mathrm{j}2\pi qf_{\mathrm{c1}}t_1}\mathrm{e}^{-\mathrm{j}(kz_{\mathrm{r1}}+q)\psi_{i1}}\delta(f-kf_{\mathrm{p1}}-qf_{\mathrm{c1}})$$
$$+\sum_{k\in z}\sum_{l\in z}\sum_{i=1}^{N_1}\gamma_l^{\mathrm{c}}\beta_k^{\mathrm{c}}\mathrm{e}^{-\mathrm{j}(kz_{\mathrm{r1}}\psi_{i1}+lz_{\mathrm{r2}}\psi_{i2})}\delta(f-kf_{\mathrm{p1}}-lf_{\mathrm{p2}}) \quad (26)$$

and the FT of equation (20) is:

$$X_2^{\mathrm{r}}(f)=\sum_{k\in z}\sum_{q\in z}\sum_{i=1}^{N_2}\alpha_q^{\mathrm{r}}\beta_k^{\mathrm{r}}\mathrm{e}^{-\mathrm{j}2\pi qf_{\mathrm{c2}}t_1}\mathrm{e}^{-\mathrm{j}(kz_{\mathrm{r2}}+q)\psi_{i2}}\delta(f-kf_{\mathrm{p2}}-qf_{\mathrm{c2}}) \quad (27)$$

The global vibration spectrum can be expressed by:

$$X^{\mathrm{c}}(f)=\sum_{k\in z}\sum_{q\in z}\sum_{i=1}^{N_1}\alpha_q^{\mathrm{c}}\beta_k^{\mathrm{c}}\mathrm{e}^{-\mathrm{j}2\pi qf_{\mathrm{c1}}t_1}\mathrm{e}^{-\mathrm{j}(kz_{\mathrm{r1}}+q)\psi_{i1}}\delta(f-kf_{\mathrm{p1}}-qf_{\mathrm{c1}})$$
$$+\sum_{k\in z}\sum_{l\in z}\sum_{i=1}^{N_1}\gamma_l^{\mathrm{c}}\beta_k^{\mathrm{c}}\mathrm{e}^{-\mathrm{j}(kz_{\mathrm{r1}}\psi_{i1}+lz_{\mathrm{r2}}\psi_{i2})}\delta(f-kf_{\mathrm{p1}}-lf_{\mathrm{p2}})$$
$$+\sum_{k\in z}\sum_{q\in z}\sum_{i=1}^{N_2}\alpha_q^{\mathrm{r}}\beta_k^{\mathrm{r}}\mathrm{e}^{-\mathrm{j}2\pi qf_{\mathrm{c2}}t_1}\mathrm{e}^{-\mathrm{j}(kz_{\mathrm{r2}}+q)\psi_{i2}}\delta(f-kf_{\mathrm{p2}}-qf_{\mathrm{c2}}) \quad (28)$$

The term $\delta(f-kf_{\mathrm{p}j}-qf_{\mathrm{c}j})$ implies that $X^{\mathrm{r}}(f)$ can take non-zero values only for the frequency $f=kf_{\mathrm{p}j}+qf_{\mathrm{c}j}$, and the term $\delta(f-kf_{\mathrm{p1}}-lf_{\mathrm{p2}})$ implies that there are components at the frequency $f=kf_{\mathrm{p1}}+lf_{\mathrm{p2}}$. The variables k and l are the tooth-meshing harmonics, and q is the sideband-harmonic.

3.3. Spectral analysis

Equation (28) implies that the structure of the vibration spectrum $X^{\mathrm{r}}(f)$ is influenced by the geometrical characteristics of the PG such as the number of planets N, the planet spacing ψ_{ij}, and the number of teeth of the ring gear $Z_{\mathrm{r}j}$.

Inalpolat and Kahraman [9] found that each geometry produced a specific spectral structure.

Molina [10] proposed that all planetary gearboxes can be classified into four groups based on their modulation activity related to two conditions, as shown in Table 1. The first condition indicates whether planets are equally or unequally spaced; this can be determined by calculating the planet spacing ψ_{ij}:

$$\psi_{ji}=\frac{2\pi(i-1)}{N} \quad (29)$$

The second condition indicates whether the planets are in phase; this can be determined by calculating the relative phase difference:

$$\gamma_{\mathrm{r}ji}=\frac{\psi_{ji}Z_{\mathrm{r}j}}{2\pi} \quad (30)$$

Table 2
Characteristics of the two-stage planetary gears.

	Sun	Ring	Carrier	Planet
Teeth number	$Z_{s1}=21$	$Z_{r1}=150$	–	$Z_{p1}=64$
	$Z_{s2}=27$	$Z_{r2}=90$	–	$Z_{p2}=31$
Mass (kg)	$M_{s1}=260$	$M_{r1}=1826$	$M_{c1}=2500$	$M_{p1}=900$
	$M_{s2}=445$	$M_{r2}=1200$	$M_{c2}=2000$	$M_{p2}=600$
J/R_{bi}^2	$\overset{1}{J}/R_{bs}^2=145.5$	$\overset{1}{J}/R_{br}^2=913$	$\overset{1}{J}/R_{bc}^2=1279$	$\overset{1}{J}/R_{bp}^2=642$
	$\overset{2}{J}/R_{bs}^2=251$	$\overset{2}{J}/R_{br}^2=650$	$\overset{2}{J}/R_{bc}^2=1050$	$\overset{2}{J}/R_{bp}^2=294$
I/R_{bi}^2	$\overset{1}{I}/R_{bs}^2=72.73$	$\overset{1}{I}/R_{br}^2=456.5$	$\overset{1}{I}/R_{bc}^2=639.5$	$\overset{1}{I}/R_{bp}^2=352.5$
	$\overset{2}{I}/R_{bs}^2=105.5$	$\overset{2}{I}/R_{br}^2=350$	$\overset{2}{I}/R_{bc}^2=550$	$\overset{2}{I}/R_{bp}^2=147$
Gearmesh stiffness (N/m)	$k_{sp1}=2\cdot10^8$, $k_{rp1}=2.3\cdot10^8$			
	$k_{sp2}=2.2\cdot10^8$, $k_{rp2}=2.3\cdot10^8$			
Bearing stiffness (N/m)	$k_{jx}=k_{jy}=10^8,\ j=\mathrm{c,s}, k_{jz}=10^9,\ j=\mathrm{c,s}$			
	$k_{rx}=k_{ry}=k_{rz}=10^{10},\ k_{xx}=k_{yy}=10^8,\ k_{zz}=10^9$			
Torsional stiffness (N/m)	$k_{j\varphi}=k_{j\psi}=10^9,\ j=\mathrm{c,s},1...n, k_{j\theta}=0,\ j=\mathrm{c,s},1...n$			
	$k_{r\varphi}=k_{r\psi}=k_{r\theta}=10^{10}$			
Pressure angle	$\alpha=20°$			
Helix angle	$\beta=20°$			

4. Results

The characteristics of the two-stage planetary gears are presented in Table 2; each one has a fixed ring and three planets [10].

The frequency analyses of the vibrations in the two different case studies of two-stage planetary gearboxes are developed. Each case presents a specific geometry, which produced a specific spectral structure.

First case study Two-stage planetary gear from group (A).

The first condition is that the planet gears of the two stages are equally spaced. Thus, $\psi_{ji}=\frac{2\pi(i-1)}{N}$ so $\gamma_{rji}=\frac{\psi_{ji}Z_{rj}}{2\pi}=\frac{Z_{rj}}{N}(i-1)$.

The second condition is that all meshes are in phase, thus γ_{rji} must be either zero or a positive integer (i.e. $\gamma_{rji}\in N$). So Z_{rj}/N must be a positive integer (i.e. $Z_{rj}/N\in N$).

The spectral structure of the vibrations is now analyzed.

The second exponential term of equations (26) and (27) can be rearranged respectively as follows:

$$e^{-j(kz_{r1}+lz_{r2}+q)\psi_{1i}}=e^{-j2\pi(i-1)[k\frac{z_{r1}}{N}+l\frac{z_{r2}}{N}+\frac{q}{N}]} \tag{31}$$

$$e^{-j(kz_{r2}+q)\psi_{2i}}=e^{-j2\pi(i-1)[\frac{kz_{r2}}{N}+\frac{q}{N}]} \tag{32}$$

with $Z_{r1}/N\in N$, $Z_{r2}/N_2\in N$ and $q\in Z$.

If q is an integer multiple of the number of planet gears N, the phases of the Nspectral components are integer multiples of 2π, which means that they are in phase. In this case, they add constructively and the component will be present in the spectrum $X_j^r(f)$ with a magnitude given by $N\alpha_q^r\beta_k^r\gamma_l^r$ for the first stage and $N\alpha_q^r\beta_k^r$ for the second one.

If q is not an integer multiple of N, the phases of the spectral components will be equally distributed in the range $[0,2\pi)$. In this case, the N spectral components add destructively and the magnitude of the component in the spectrum is zero.

So, the spectral structure consists of components at the gear mesh frequency of the second stage and its multiples modulated by sidebands spaced by Nf_{c2}, and components at the gear mesh frequency of the first stage and its multiples modulated by sidebands spaced by Nf_{c1} and other sidebands spaced by f_{p2}. So:

$$X_1^c(f)=\begin{Bmatrix} N\alpha_q^c\beta_k^c\gamma_l^c e^{-j2\pi qf_{c1}t_{11}}\delta(f-kf_{m1}-qf_{c1})+N\beta_k^c\gamma_l^c\delta(f-kf_{p1}-lf_{p2}) & \text{if } \frac{q}{N}\in N \\ N\beta_k^c\gamma_l^c\delta(f-kf_{p1}-lf_{p2}) & \text{otherwise} \end{Bmatrix} \tag{33}$$

$$X_2^r(f)=\begin{Bmatrix} N\alpha_q^r\beta_k^r e^{-j2\pi qf_{c2}t_{12}}\delta(f-kf_{p2}-qf_{c2}) & \text{if } \frac{q}{N}\in N \\ 0 & \text{otherwise} \end{Bmatrix} \tag{34}$$

So, the global spectrum is:

$$X^r(f)=X_1^r(f)+X_2^r(f) \tag{35}$$

Fig. 3 illustrates the spectrum of Eq. (35) for a two-stage planetary gear with three planets, each one with $Z_{r1}=150$ and $Z_{r2}=90$. The mesh frequency for the first stage of the planetary gear is $f_{p1}=132$ Hz and the mesh frequency for the

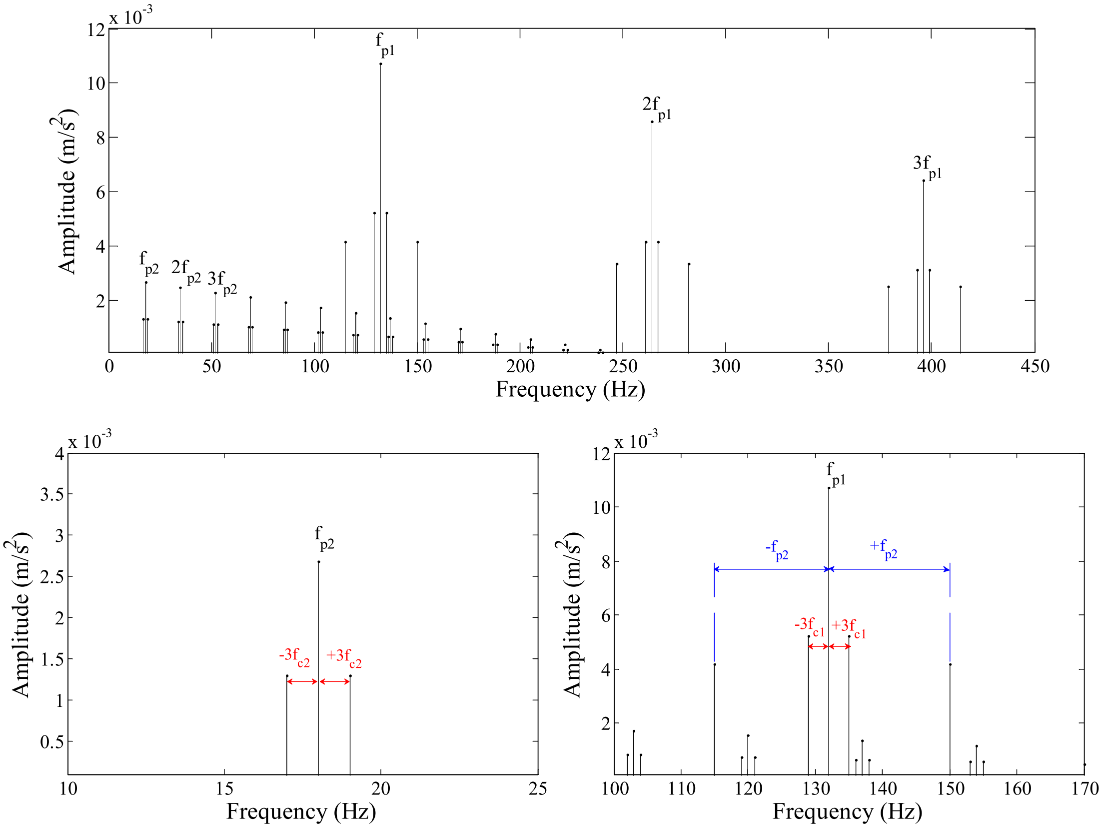

Fig. 3. Spectral structure of a two-stage planetary gear from group (A) with three equally spaced planets ($Z_{r1} = 150$, $Z_{r2} = 90$ and $\psi_{ji} = \{0, \frac{2\pi}{3}, \frac{4\pi}{3}\}$).

second stage is $f_{p2} = 18$ Hz. The rotational frequency of the carrier of the first stage is $f_{c1} = 0.88$ Hz and that of the second stage is $f_{c2} = 0.2$ Hz.

In order to take into account the influence of the sensor in the numerical simulation, a Hanning function is used to represent this phenomenon [9]; it can be expressed by:

$$w(t) = \frac{1}{2} - \frac{1}{2}\left[\cos\left(\frac{2\pi N t}{T_c}\right)\right] \tag{36}$$

With this, for a planet positioned at angle ψ_i, a weighting function is defined as:

$$w_i(t) = W_i w\left(t - \frac{\psi_i}{2\pi} T_c\right) U_i(t) \tag{37}$$

where $U_i(t)$ is defined as:

$$U_i(t) = \sum_{n=1}^{\infty} \left\{ u\left[t - \left(\frac{(n-1)N + i - 1}{N}\right) T_c\right] - u\left[t - \left(\frac{(n-1)N + i}{N}\right) T_c\right]\right\} \tag{38}$$

In this equation, the terms $u\ (t - a)$ are unit step functions ($u(t - a) = 1$ for $t > a$ and $u(t - a) = 0$ for $t < a$), which ensures the influence of planet i on the sensor for a period T_c/N.

The dynamic force due to the rotation of the carrier will be:

$$F_j(t) = \sum_{i=1}^{N} w_{ij}(t) U_{ij}(t) F_{ij} \cos(Z_r w_c t + Z_r \psi_{ij}) \tag{39}$$

where $j = 1$ for the first stage and $j = 2$ for the second one. F_{ij} is the load-sharing planet-ring.

Fig. 4 presents the spectrum obtained by numerical simulation using the implicit Newmark's time-step integration of the lumped parameters model for the same gearbox. The same observation as that found in the spectrum obtained by the phenomenological model (Fig. 3) can be made.

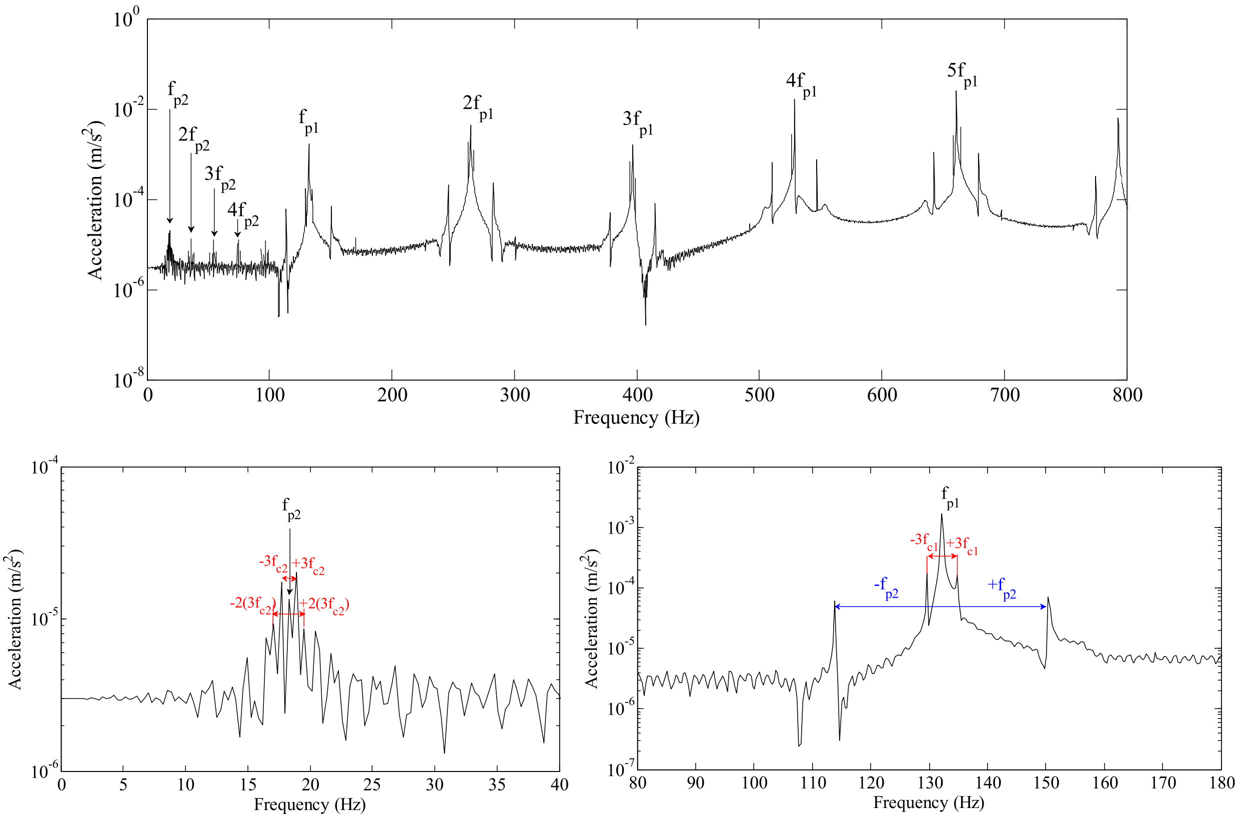

Fig. 4. Results of the numerical simulation of a two-stage planetary gear from group (A) with three equally spaced planets ($Z_{r1} = 150$, $Z_{r2} = 90$ and $\psi_{ji} = \{0, \frac{2\pi}{3}, \frac{4\pi}{3}\}$).

Table 3
Phase of term (I) in Eq. (40).

k	Phase expression	Phase in the range $[0, 2\pi)$		
		$i = 1$	$i = 2$	$i = 3$
1	$2\pi\ (i-1)\ 152/3$	0	$\frac{2}{3}2\pi$	$\frac{1}{3}2\pi$
2	$4\pi\ (i-1)\ 152/3$	0	$\frac{1}{3}2\pi$	$\frac{2}{3}2\pi$
3	$6\pi\ (i-1)\ 152/3$	0	0	0

Second case study First stage of the planetary gear from group (B) and second stage from group (A).

In this part, the first stage of the planetary train belongs to group (B), so it still has equally spaced planet gears, but the meshing processes are no longer in phase. As a result, Z_{r1}/N is no longer an integer.

In order to explain these observations, we consider a first-stage planetary gear with three planets and $Z_{r1} = 152$ (Z_{c1}/N is not an integer), and the meshing frequency takes the value $f_{p1} = 132.5$ Hz, and the rotational frequency of the carrier is $f_{c1} = 0.87$ Hz, the second stage have the same characteristics as in the preceding example ($f_{p2} = 18$, $f_{c2} = 0.2$).

The second exponential term of equation (26) can be arranged in the following way:

$$e^{-j(kZ_{c1}+q)\psi_{1i}} = \underbrace{e^{-j2\pi(i-1)k\frac{Z_{c1}}{N}}}_{\text{I}} \underbrace{e^{-j2\pi(i-1)\frac{q}{N}}}_{\text{II}} \tag{40}$$

$$e^{-j(kZ_{c1}+lZ_{c2})\psi_{i}} = \underbrace{e^{-j2\pi(i-1)k\frac{Z_{c1}}{N}}}_{\text{I}} \underbrace{e^{-j2\pi(i-1)l\frac{Z_{c2}}{N}}}_{\text{III}} \tag{41}$$

It is observed that the phase of term (I) in Eq. (40) depends on the values of i and k, while the phase of term (II) depends on the values of i and q and the phase of term (III) in Eq. (41) depends on the values of i and l.

Tables 3, 4 and 5 show, respectively, the phase in the range $[0, 2\pi)$ of the term (I), (II) and (III), for the N components, for $k > 0$, $-3 \le q \le 3$ and $l > 0$.

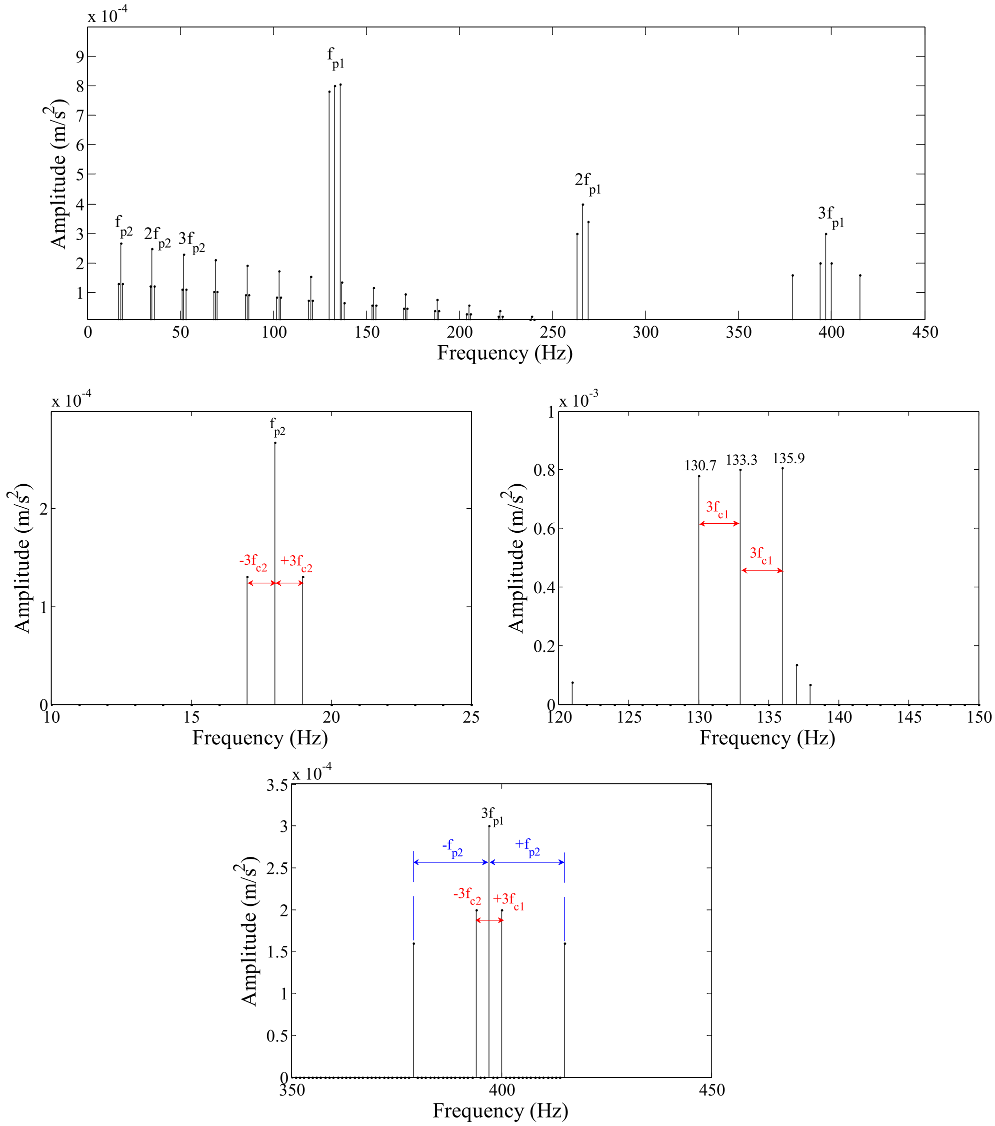

Fig. 5. Spectral structure of two stages planetary gear with 3 planets, the first stage from group (B) and the second one from group (A) ($Z_{r1} = 152$, $Z_{r2} = 90$ and $\psi_{ji} = \{0, \frac{2\pi}{3}, \frac{4\pi}{3}\}$).

Table 4
Phase of term (II) in Eq. (40).

q	Phase expression	Phase in the range $[0, 2\pi)$		
		$i = 1$	$i = 2$	$i = 3$
-3	$-6\pi\ (i-1)/3$	0	0	0
-2	$-4\pi\ (i-1)/3$	0	$\frac{1}{3}2\pi$	$\frac{2}{3}2\pi$
-1	$-2\pi\ (i-1)/3$	0	$\frac{2}{3}2\pi$	$\frac{1}{3}2\pi$
0	0	0	0	0
1	$2\pi\ (i-1)/3$	0	$\frac{1}{3}2\pi$	$\frac{2}{3}2\pi$
2	$4\pi\ (i-1)/3$	0	$\frac{2}{3}2\pi$	$\frac{1}{3}2\pi$
3	$6\pi\ (i-1)/3$	0	0	0

The presence of the component at the frequency $f = kf_{m1} + qf_{c1}$ in the spectrum $X_1^{\mathrm{r}}(f)$ is evaluated by adding the phases of term (I) and term (II) and the presence of the component at the frequency $f = kf_{p1} + lf_{p2}$ is evaluated by adding the phases of term (I) and term (III).

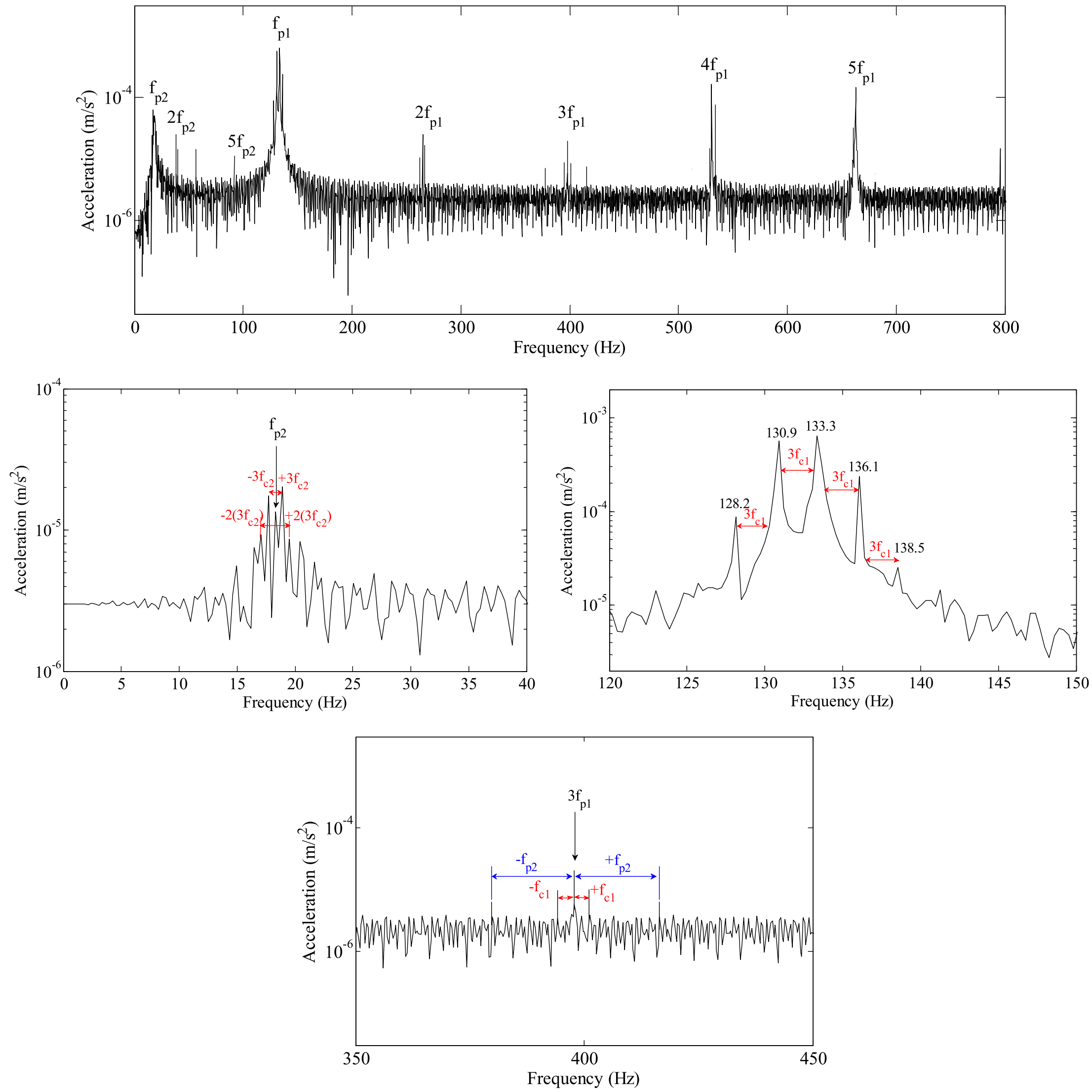

Fig. 6. Results of the numerical simulation of a two-stage planetary gear with three planets, the first stage from group (B) and the second one from group (A) ($Z_{r1} = 152$, $Z_{r2} = 90$ and $\psi_{ji} = \{0, \frac{2\pi}{3}, \frac{4\pi}{3}\}$).

Table 5
Phase of term (III) in Eq. (41).

l	Phase expression	Phase in the range $[0, 2\pi)$		
		$i = 1$	$i = 2$	$i = 3$
1	$2\pi\ (i-1)\ 90/3$	0	0	0
2	$4\pi\ (i-1)\ 90/3$	0	0	0
3	$6\pi\ (i-1)\ 90/3$	0	0	0

For example, for the component at the gear mesh frequency $f = f_{p1}$ (i.e. $k = 1$; $q = 0$), the phase of the N components is $\{0 + 0, \frac{2}{3}2\pi + 0, \frac{1}{3}2\pi + 0\} = \{0, \frac{2}{3}2\pi, \frac{1}{3}2\pi\}$, which means that they are equally distributed in the range $[0, 2\pi)$. So, they add destructively and the magnitude of the component at $f = f_{p1}$ is zero.

Now, for the component at the frequency $f = f_{p1} + f_{c1}$ (i.e. $k = 1$; $q = 1$), the phase of the N components is $\{0 + 0, \frac{2}{3}2\pi + \frac{1}{3}2\pi, \frac{1}{3}2\pi + \frac{2}{3}2\pi\} = \{0, 0, 0\}$, which means that they are in phase, so they add constructively and the component at $f = f_{p1} + f_{c1}$ is present in the spectrum.

So, from the values given in Tables 3 and 4, the following combinations of $(k; q)$ give a constructive sum: $(1, -2)$, $(1, 1)$, $(2, -1)$, $(3, -3)$, $(3, 0)$, $(3, 3)$ and from Tables 4 and 5, the following combinations of (k, l) give a constructive sum: $(3, 1)$, $(3, 2)$, $(3, 3)$.

Consequently, in the global spectrum, there is no component at the gear mesh frequency of the first-stage planetary gear and its harmonics. It presents an asymmetrical distribution of components in frequency and amplitude spaced by Nf_{c1}. But there is a component at the Nth harmonic of the meshing frequency modulated by symmetrical sidebands spaced by f_{p2}. The global spectral structure has also components at the meshing frequency of the second stage and its harmonics, each with symmetrical sidebands spaced by Nf_{c2}.

Fig. 5 shows the global spectrum of these two stages.

Fig. 6 presents the spectrum obtained by numerical simulation for the same gearbox. One can observe the same component as that in the spectrum obtained by the phenomenological model (Fig. 5).

5. Conclusion

Two models of two-stage planetary gearbox are adopted to describe vibrations: (*i*) the lumped-parameter model, which is based on the numerical solution to the equations of motion and describes the vibrations with respect to a rotating reference frame, and (*ii*) the phenomenological model, which describes the vibrations of the ring gear with respect to an inertial reference frame, and takes into account the influence of the sensor. The results from the lumped-parameter model are transferred into an inertial reference frame by including the amplitude modulation effect due to the variable transmission path. Different spectral structures are found. Based on this, planetary gearboxes are classified in four groups, each one presenting a specific geometry and a specific spectral structure. Both models are developed for a two-stage planetary gear. Two different case study of two-stage planetary gear are adopted to describe the vibration behavior and the corresponding spectrum, which show close agreement between the two models. The presence of the characteristic frequencies of the two stages planetary gears such as the gearmesh frequencies and the carrier rotation frequencies is noticed. Each gearmesh frequency is modulated by the carrier rotation frequency of the same stage. One can observe also the interaction between the two stages of the planetary gear, which is evidenced through the modulation of the first-stage gearmesh frequency by the second one.

Depending on the geometry of the planetary gear, a specific spectral structure is observed, which is characterized by a symmetrical and/or asymmetrical distribution of its components.

References

[1] F. Cunliffe, J.D. Smith, D.B. Welbourn, Dynamic tooth loads in epicyclic gears, J. Eng. Ind. 94 (1974) 578–584.
[2] A. Saada, P. Velex, An extended model for the analysis of the dynamic behavior of planetary trains, J. Mech. Des. 117 (1995) 241–247.
[3] J. Lin, R. Parker, Structured vibration characteristics of planetary gears with unequally spaced planets, J. Sound Vib. 233 (2000) 921–928.
[4] F. Chaari, M. Haddar, Dynamic analysis of a planetary gear failure caused by tooth pitting and cracking, Eng. Fail. Anal. 2 (2005) 73–78.
[5] F. Chaari, W. Baccar, M. Haddar, Effect of spalling or tooth breakage on gearmesh stiffness and dynamic response of a one-stage spur gear transmission, Eur. J. Mech. A, Solids 27 (2008) 691–705.
[6] J. Lin, R. Parker, Mesh phasing relationships in planetary and epicyclic gears, J. Mech. Des. 126 (2004) 365–370.
[7] P. McFadden, J. Smith, An explanation for the asymmetry of the modulation sidebands about the tooth meshing frequency in epicyclic gear vibration, Proc. Inst. Mech. Eng. 199 (1985) 65–70.
[8] J. McNames, Fourier series analysis of epicyclic gearbox vibration, J. Vib. Acoust. 124 (2002) 150–152.
[9] M. Inalpolat, A. Kahraman, A theoretical and experimental investigation of modulation sidebands of planetary gear sets, J. Sound Vib. 323 (2009) 677–696.
[10] C. Molina Vicuna, Contributions to the Analysis of Vibrations and Acoustic Emissions for the Condition Monitoring of Epicyclic Gearboxes, Dissertation, Faculty of Georesources and Materials Engineering of the RWTH Aachen University, Germany, 2009.
[11] P. Samuel, J. Conroy, D. Pines, Planetary Transmission Diagnostics, Technical Report NASA/CR 2004 213068, NAS, 2004.
[12] J. Thomas, A Procedure for Predicting the Load Distribution and Transmission Error Characteristics of Double Helical Gears, MS Thesis, The Ohio State University, 1991.
[13] L. Zhang, Y. Wang, K. Wu, R. Sheng, Q. Huang, Dynamic modeling and vibration characteristics of a two-stage closed-form planetary gear train, Mech. Mach. Theory 97 (2016) 12–28.
[14] M. Karray, N. Feki, M.T. Khabou, H. Chaari, M. Haddar, Modal analysis of gearbox transmission system in bucket wheel excavator, J. Theor. Appl. Mech. 55 (1) (2017) 253–264.
[15] A. Kahraman, Planetary gear train dynamics, ASME J. Mech. Des. 116 (1994) 713–720.
[16] P. Velex, Contribution à l'analyse du comportement dynamique de réducteur à engrenages à axes parallèles, PhD thesis, Institut national des sciences appliquées de Lyon, Villeurbanne, France, 1988, 188 p.
[17] M. Karray, N. Feki, M.T. Khabou, H. Chaari, M. Haddar, Dynamic analysis of bevel gear coupled to multiple stage planetary gear (excavator system), in: Proc. 6th International Conference on Advances in Mechanical Engineering and Mechanics, ICAMEM'2015, 20–22 December 2015, Hammamet, Tunisia, 2015.
[18] W. Bartelmus, Mathematical modeling and computer simulations as an aid to gearbox diagnostics, Mech. Syst. Signal Process. 15 (5) (2001) 855–871.